ISBN: 978-3-95450-241-7 ISSN: 2673-5350 doi:10.18429/JACoW-IBIC2022-MOP27

DESIGN CONSIDERATIONS OF THE CORRUGATED STRUCTURES IN A VACUUM CHAMBER FOR IMPEDANCE STUDIES AT KARA

S. Maier*, M. Brosi†, H. J. Cha, A. Mochihashi, M. J. Nasse, P. Schreiber, M. Schwarz, A.-S. Müller
Karlsruhe Institute of Technology, Karlsruhe, Germany

Abstract

Two parallel, corrugated plates will be installed at the KIT storage ring KARA (KArlsruhe Research Accelerator). This impedance manipulation structure can be used to study and eventually control the electron beam dynamics and the emitted coherent synchrotron radiation (CSR) at KARA. In this contribution, we present the design of the impedance manipulation structure with corrugated plates, simulation results showing the influence of different corrugation parameters on its impedance, and the impact of this additional impedance source on the temporal changes in the emitted CSR in the presence of the microbunching instability.

INTRODUCTION

Unlike the incoherent synchrotron radiation, the coherent synchrotron radiation (CSR) does not scale linearly but quadratically with the number of emitting particles, so consequently the emitted photon flux can be enhanced by multiple orders of magnitude, for typical electron synchrotron radiation facilities. This makes it attractive to use the CSR for various kinds of applications. However, the emitted radiation is only coherent when its wavelength is longer than the emitting structure. Therefore, very short bunches and thus a high particle density is required to extend the CSR to a higher frequency range and to increase the total radiation intensities. In such a short-bunch regime, collective phenomena occur due to an interaction of an electron bunch with its own self-emitted CSR, which can lead to bunch deformations and dynamic instabilities like the so-called microbunching instability [1]. Especially, the microbunching instability leads to dynamically changing substructures and thereby intermittent regions of increased longitudinal charge density causing intense bursts of CSR in the THz frequency range.

A versatile impedance manipulation chamber is in development and will be installed into the KIT storage ring, KARA. The purpose of this chamber is to study the effect on the microbunching instability by manipulating the longitudinal impedance and thereby affecting the longitudinal beam dynamics of the electron bunches. The additional impedance is generated by a pair of horizontal, parallel plates with periodic, rectangular corrugations. Figure 1 shows a schematic drawing with the parameters corrugation depth h, corrugation width g, periodic length L, and plate distance $2b$. A cylindrical corrugated pipe has been tested in a linear accelerator by Bane *et al.* [2, 3], where they produced narrow-banded THz pulses of Smith-Purcell radiation [4], which is not examined in the KARA project. To our knowledge, such a structure has not yet been tested in a storage ring, where the wakefields in the corrugated structure can affect frequently the bunch profile and the resulting CSR due to the passing of the structure with a revolution frequency of 2.7 MHz (for KARA).

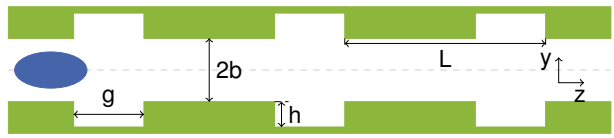

Figure 1: The corrugated pipe in cross section with the relevant geometric parameters corrugation depth h, corrugation width g, periodic length L, and plate distance $2b$ is shown. The electron bunch is indicated in blue.

The longitudinal impedance $Z^{\parallel}$ of a cylindrical, corrugated pipe has been theoretically described in Ng *et al.* [5] with the validity range $L \lesssim h \ll b$, as

$$\frac{Z^{\parallel}}{L} = \frac{Z_{\mathrm{vac}}}{\pi b^2}\left[\pi k_{\mathrm{res}}\delta\left(k^2 - k_{\mathrm{res}}^2\right) + i \cdot \mathrm{P.V.}\left(\frac{k}{k^2 - k_{\mathrm{res}}^2}\right)\right] \quad (1)$$

with the resonance wave number $k_{\mathrm{res}} = \sqrt{\frac{2L}{bgh}}$, the wave number $k = \frac{\omega}{c}$, the vacuum impedance $Z_{\mathrm{vac}} \simeq 377\,\Omega$, the δ-distribution, and the principal value $\mathrm{P.V.}(x)$ [6].

At KARA, the CSR impedance is the dominant longitudinal impedance source in the short-bunch operation mode at 1.3 GeV. In the frequency range below 200 GHz, the parallel plate impedance gives for the impedance per revolution the highest contribution with up to 10 kΩ and thus an additional impedance of 1 kΩ, which can be generated by the corrugated structure, could significantly contribute to the total impedance. For now, the parameter values of the corrugations in Table 1 were chosen so that the theoretical resonance frequency $f_{\mathrm{res}} = \frac{c}{2\pi}k_{\mathrm{res}}$ lies between 50 GHz and 200 GHz. The simulated impedance can be described by an effective resonator model [7] that is characterized by the resonance frequency f_{res}, the shunt impedance Z_0, and the quality factor Q.

Table 1: Parameter Values Used for the Simulations

Parameter	Variable	Range
Periodic length	L	50 µm to 200 µm
Corrugation depth	h	50 µm to 300 µm
Corrugation width	g	12.5 µm to 150 µm

* sebastian.maier@kit.edu
† Now at MAX IV Laboratory, Lund, Sweden

Content from this work may be used under the terms of the CC BY 4.0 licence (© 2022). Any distribution of this work must maintain attribution to the author(s), title of the work, publisher, and DOI

ISBN: 978-3-95450-241-7 ISSN: 2673-5350 doi:10.18429/JACoW-IBIC2022-MOP27

To determine the smallest possible plate distance for experiments, a set of two vertical scrapers were moved towards the beam from the top and the bottom. This experiment, in the short-bunch operation mode, showed a drastic reduction of the beam lifetime due to a significant loss of electrons for a vertical opening of $b_{\mathrm{Scraper}} \leq 3\,\mathrm{mm}$. Based on this and taking into account the different value of the vertical beta-function at the position of the scraper and the planned chamber, $b = 5\,\mathrm{mm}$ was chosen as the smallest plate distance for the simulations. In the following, if not explicitly stated otherwise, the duty-cycle of the corrugations is taken to be 50% or rather $L/g = 2$. At KARA, a limited space of around 48 cm is available in the ring for the entire chamber including taper sections and vacuum pumps. Therefore, the length of the corrugated structure is limited to 20-25 cm, but in this paper a length of $s = 10\,\mathrm{cm}$ was chosen to reduce the simulation time. In contrast to Ref. [8], design considerations of the corrugated plates will now also be discussed in this contribution.

IMPEDANCE SIMULATION

To simulate the impedance of the corrugated structures, the Wakefield solver of the CST Particle Studio [9] was used. Its numerical code computes the wakefields in the time domain and calculates the impedance from the Fourier transformation of the longitudinal wake potential and the Fourier transformed charge distribution of the bunch. The simulated structure consists of two corrugated plates of stainless steel and vacuum between them. A more detailed description of the settings for the impedance simulations is given in Ref. [10].

Plate Distance

The impact of the plate distance $2b$ on the impedance is of great importance for the chamber design because of the need to be able to remove the additional impedance for the normal KARA machine operation. Furthermore it is a tuning knob during the experiments as the parameters of the corrugation structures are typically fixed. The variation of the real part of the longitudinal impedance of a corrugated structure with the half plate distance b is shown in Fig. 2. The increase of the plate distance results in a distinct reduction of the magnitude of the impedance, as expected from Eq. (1).

Figure 3 shows the shunt impedance Z_0 for different b, fixed $h = 200\,\mu\mathrm{m}$ and $L = 100\,\mu\mathrm{m}$. From Eq. (1) we would expect a $1/b^{5/2}$ dependency based on the pre-factors of the δ-function. From the fit, however, we find a $1/b^{\gamma}$ with $\gamma = 2.23 \pm 0.02$ behavior with an exponent smaller than predicted for a cylindrical corrugated pipe in the equation. The deviation might be explained by the different geometric shape of the structure (parallel corrugation plates). Furthermore, the simulation results showed that the exponent was not constant for different corrugation parameters and increased with both L and h.

Figure 2 also shows that f_{res} is not nearly as strongly affected by plate distance as Z_0, but is rather determined by

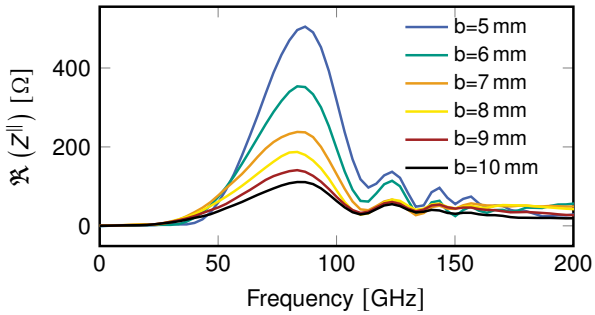

Figure 2: Real part of the longitudinal impedance $Z^{\parallel}$ for different half plate distances b and a fixed corrugation depth $h = 200\,\mu\mathrm{m}$ and periodic length $L = 100\,\mu\mathrm{m}$, respectively.

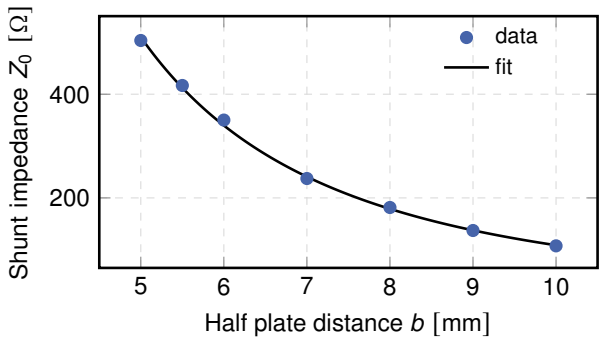

Figure 3: Shunt impedance Z_0 in dependence of the half plate distance b. The parameters of the corrugations are the same as in Fig. 2. The fit validates the $1/b^{\gamma}$ behaviour with $\gamma = 2.23 \pm 0.02$.

the corrugation parameters [10]. This gives the possibility to manipulate the strength of the influence of an additional impedance without significantly affecting other characteristics of the impedance.

Plate Width

In the case of a narrow transverse width of the corrugated plate, the side edges could affect the impedance. To determine the required width, to avoid effects of the lateral edges of the corrugated plate on the impedance, simulations as a function of the plate width x_0 of the corrugated structure were done. The real part of the longitudinal impedance for a corrugated structure with the parameters $h = 200\,\mu\mathrm{m}$ and $L = 100\,\mu\mathrm{m}$ for different plate widths x_0 is shown in Fig. 4. It can clearly be seen that for narrower corrugated plates not only the strength of the impedance is suppressed but also f_{res} is shifted. Above a width of x_0 =16 mm, it seems that the impedance characteristics remain nearly unchanged. In Fig. 5 the impedance parameters Z_0 and f_{res} - determined by fit - are shown in dependency of the plate width. In the case of $x_0 \leq 10\,\mathrm{mm}$, the shunt impedance increases roughly linearly with x_0 before it seems to approach a level of saturation to an asymptotic limit, which is assumed to be reached at $x_0 \geq 16\,\mathrm{mm}$. Moreover, the resonance frequency reaches the asymptotic limit for the same width x_0 of the corrugated structure, so this could be defined as the minimum necessary width.

Content from this work may be used under the terms of the CC BY 4.0 licence (© 2022). Any distribution of this work must maintain attribution to the author(s), title of the work, publisher, and DOI

ISBN: 978-3-95450-241-7 ISSN: 2673-5350 doi:10.18429/JACoW-IBIC2022-MOP27

Content from this work may be used under the terms of the CC BY 4.0 licence (© 2022). Any distribution of this work must maintain attribution to the author(s), title of the work, publisher, and DOI

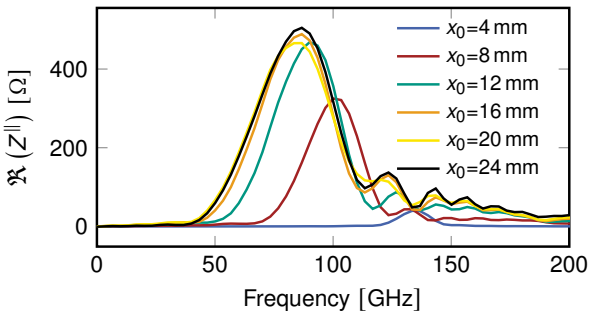

Figure 4: Real part of the longitudinal impedance $Z^{\parallel}$ for a different width x_0 of the corrugated plate with a fixed corrugation depth $h = 200\,\mu\text{m}$ and periodic length $L = 100\,\mu\text{m}$, respectively.

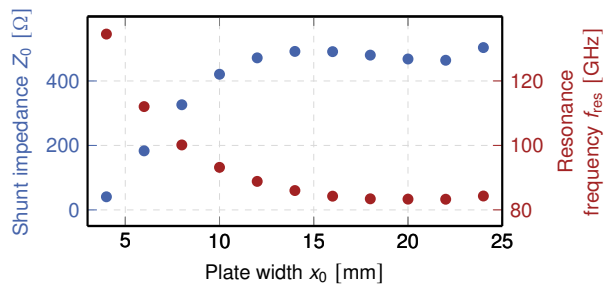

Figure 5: Shunt impedance Z_0 (blue) and resonance frequency f_{res} (red) in dependence of the width x_0 of the corrugated plate for a fixed corrugation depth $h = 200\,\mu\text{m}$ and periodic length $L = 100\,\mu\text{m}$, respectively.

However, the horizontal dimension of the bunch ($\sigma_x \approx 0.5$ mm) as well as the horizontal orbit in the section of the impedance chamber need to be taken into account. Therefore we chose $x_0 = 20$ mm as the realistic width. This relatively narrow width compared to the normal KARA vacuum chamber width of $x_{\text{KARA}} = 70$ mm makes it possible to mount three independent strips with different corrugation parameters next to each other. This allows switching between different corrugations without breaking the vacuum in the chamber. By moving the corrugation plates with the three strips horizontally, the active strip interacting with the electron bunch can be chosen by centering the strip over the bunch orbit. However, since one strip is required as a reference strip without any corrugations, only two strips with different corrugations can be installed. By moving the corrugated plates vertically far enough apart ($2b = 32$ mm) the normal KARA beam pipe cross section can be imitated, practically disabling the additional corrugation impedance.

To find the structure parameters and the resulting impedance that efficiently affect the microbunching instability, beam dynamic simulations have been performed, which are described in the following section.

BEAM DYNAMICS SIMULATION

The beam dynamics simulations were done with the in-house developed Vlasov-Fokker-Planck solver, Inovesa [11], which can reproduce the longitudinal beam dynamics during the microbunching instability observed at KARA [12]. For the studies presented here, settings that match the short-bunch operation mode at KARA with a synchrotron frequency $f_{\text{sync}} = 9.44$ kHz, the acceleration voltage $V_{\text{RF}} = 1.048$ MV, and the zero-current bunch length $\sigma_{z,0} = 4.1$ ps at a beam energy of $E = 1.3$ GeV were used for Inovesa. The total impedance is defined as a sum of the dominant CSR parallel plate impedance [13] and the additional impedance of the corrugated plates. The former was shown to drive the microbunching instability [12, 14] at KARA. The corrugated plate impedance is described and given by the resonator model and its parameters f_{res}, Z_0, and Q.

Threshold Current & Bursting Frequency

The CST impedance simulations have shown that for a plate distance of $b = 5$ mm and a structure length of 20 cm the impedance parameters $Q = 3$ and $Z_0 = 1\,\text{k}\Omega$ can be realized. In Ref. [8] we have already presented the results of Inovesa beam dynamics simulations directly above and below the unperturbed microbunching bursting threshold current I_{thr} with additional corrugated plate impedances, with varying f_{res}. The bursting threshold current is the limit, above which the first fluctuations in the intensity of the CSR occur. Below the threshold current, the fluctuation power at the bursting frequency, which is the dominant frequency of the intensity fluctuation of the CSR caused by microbunching, is drastically reduced in amplitude [15]. So this parameter can be used to determine the bursting threshold current.

Preliminary studies showed that impedances with $f_{\text{res}} = 110$ GHz and $f_{\text{res}} = 180$ GHz affect the fluctuation power of the emitted CSR particularly for the used typical KARA parameters. Hence, we simulated the beam dynamics for these two settings in detail by calculating so-called spectrograms with Inovesa. The results for these two cases, together with the case without additional impedance as reference are shown in Fig. 6. A spectrogram is the Fourier transform of the emitted CSR time-domain signal as function of bunch current showing the fluctuation frequency of the emitted radiation intensity. It indicates the dominant frequencies caused by microbunching. For the current range directly above the threshold this results in a finger-like structure, that is characteristic of the microbunching-induced beam dynamics directly above the threshold current [14, 16].

It can be seen that the general "shape" of this finger is not changed significantly by an additional corrugated plate impedance with $Z_0 = 1\,\text{k}\Omega$. However, the two different impedances affect the characteristic parameters of the finger, namely the threshold current I_{thr} and the bursting frequency at the threshold f_{burst}. This shows that the longitudinal beam dynamics is modified by the additional impedance in comparison to the pure CSR impedance case.

For the $f_{\text{res}} = 110$ GHz impedance the threshold current is reduced significantly by 16 µA (7.1%), whereas the bursting frequency at the threshold is not changed. In contrast,

ISBN: 978-3-95450-241-7 ISSN: 2673-5350 doi:10.18429/JACoW-IBIC2022-MOP27

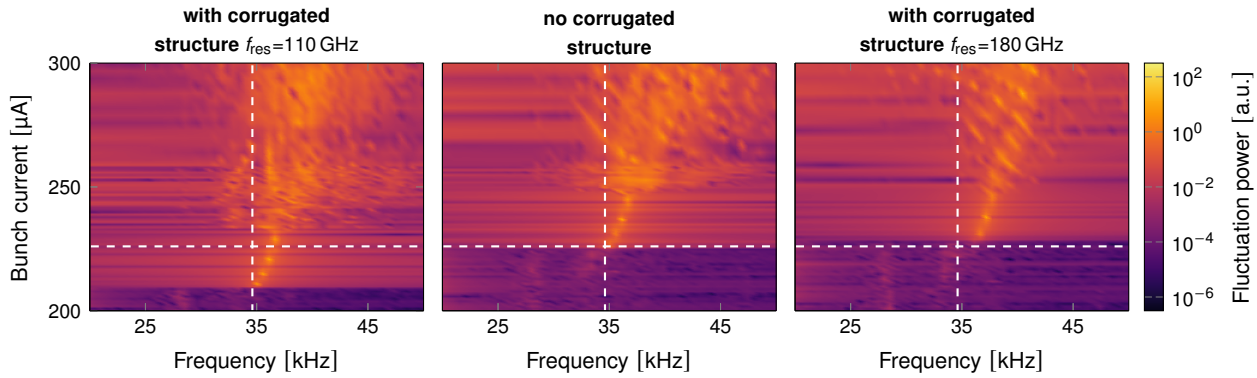

Figure 6: Color-coded power of the emission fluctuations as a function of the fluctuation frequency around the bursting frequency f_{burst} as a scan over the bunch current with and without additional corrugation impedances for two resonance frequencies f_{res}.The shunt impedance and quality factor were fixed at $Z_0 = 1\,\mathrm{k\Omega}$ and $Q = 3$, respectively. The white dashed lines mark the onset of the fluctuations due to the microbunching and the corresponding bursting frequency in the case without the corrugated structure (center).

for a corrugation impedance with $f_{\mathrm{res}} = 180\,\mathrm{GHz}$ the threshold current is increased slightly by 3 μA, so that the CSR outbursts and the emission of intense THz radiation are suppressed for a somewhat larger current range. Additionally, in this case the bursting frequency increased by 1.9 kHz.

Figure 7 illustrates how both threshold parameters develop for the two impedance configurations in dependence on the shunt impedance. This shows that depending on the chosen f_{res} of the additional impedance, one threshold parameter changes significantly and almost linearly with increasing shunt impedance, whereas the other parameter remains nearly unchanged.

SUMMARY & OUTLOOK

It is planned to install a chamber with two horizontal, parallel plates with corrugated structures into the KARA storage ring to study and manipulate the microbunching instability. The impedance simulations showed that the possibility of changing the distance between the plates and the electron beam offers a tuning knob to change the shunt impedance during operation. Furthermore, it is planned to mount three strips with a width of $x_0 = 20\,\mathrm{mm}$ nearby each other on a plate so that different structures can be tested without breaking the vacuum. The current plan is, that two strips will have corrugations producing an impedance with a resonance frequency of $f_{\mathrm{res}} = 110\,\mathrm{GHz}$ and $f_{\mathrm{res}} = 180\,\mathrm{GHz}$, respectively. The remaining strip will not have any corrugations to separate the influence of the corrugated structure from the change of the geometric aperture of the beam pipe.

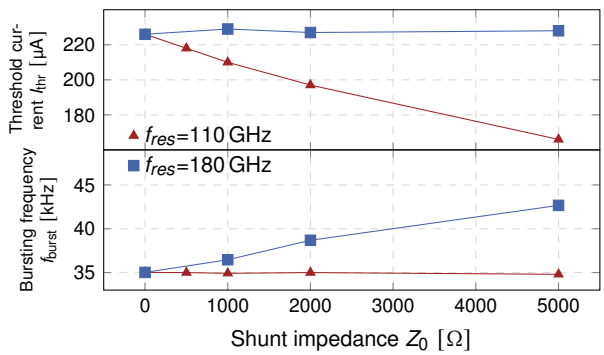

Figure 7: Bursting threshold and frequency for different shunt impedances Z_0. An additional impedance with a resonance frequency $f_{\mathrm{res}} = 180\,\mathrm{GHz}$ (blue) affects the bursting frequency, whereas $f_{\mathrm{res}} = 110\,\mathrm{GHz}$ (red) changes the threshold current.

Beam dynamics studies with the Vlasov-Fokker-Planck solver Inovesa, indicate that the resonance frequency is the crucial parameter of the additional impedance, which decides in what way the microbunching instability is influenced. This parameter decides whether the bursting threshold is reduced (and thus intensive THz radiation is emitted at even lower currents), or the dominant fluctuation frequency in the emitted CSR intensity is changed.

As a next step, the corrugated plate will be manufactured and the chamber details will be determined. A key challenge is to design a short taper section that allows both vertical and horizontal movement of the corrugated plates.

ACKNOWLEDGEMENTS

This work is supported by the DFG project 431704792 in the ANR-DFG collaboration project ULTRASYNC.

S. Maier and P. Schreiber acknowledge the support by the Doctoral School „Karlsruhe School of Elementary and Astroparticle Physics: Science and Technology“ (KSETA).

REFERENCES

[1] A.-S. Müller *et al.*, “Far Infrared Coherent Synchrotron Edge Radiation at ANKA”, in *Proc. PAC'05*, Knoxville, TN, USA, May 2005, paper RPAE038, pp. 2518-2520. https://jacow.org/p05/papers/rpae038.pdf

[2] K. L. F. Bane and G. Stupakov, “Terahertz radiation from a pipe with small corrugations”, *Nucl. Instrum. Methods Phys. Res., Sect. A*, vol. 677, pp.67-73, 2012. doi:10.1016/j.nima.2012.02.028

Content from this work may be used under the terms of the CC BY 4.0 licence (© 2022). Any distribution of this work must maintain attribution to the author(s), title of the work, publisher, and DOI

ISBN: 978-3-95450-241-7 ISSN: 2673-5350 doi:10.18429/JACoW-IBIC2022-MOP27

Content from this work may be used under the terms of the CC BY 4.0 licence (© 2022). Any distribution of this work must maintain attribution to the author(s), title of the work, publisher, and DOI

[3] K. L. F. Bane *et al.*, "Measurement of terahertz radiation generated using a metallic, corrugated pipe", *Nucl. Instrum. Methods Phys. Res., Sect. A*, vol. 844, pp.121-128, 2017. doi:10.1016/j.nima.2016.11.041

[4] S. J. Smith and E. M. Purcell, "Visible Light from Localized Surface Charges Moving across a Grating", *Phys. Rev.*, vol. 92, no. 4, 1953. doi:10.1103/PhysRev.92.1069

[5] K. Y. Ng *et al.*, "Explicit expressions of impedances and wake functions", Fermi National Accelerator Lab. (FNAL), Batavia, IL, USA, 2010.

[6] V. S. Vladimirov, *Equations of Mathematical Physics*, New York, NY, USA: M. Dekker, 1971, p.75

[7] K. Y. Ng, "Impedances of bellow corrugations", Fermi National Accelerator Lab. (FNAL), Batavia, IL, USA, 1987.

[8] S. Maier *et al.*, "Simulation of the Effect of Corrugated Structures on the Longitudinal Beam Dynamics at KARA", in *Proc. IPAC'22*, Bangkok, Thailand, June 2022, pp. 2241-2244. doi:10.18439/JACoW-IPAC2022-WEPOMS006

[9] CST Studio Suite, Dassault Systèmes, https://www.cst.com

[10] S. Maier *et al.*, "Impedance Studies of a Corrugated Pipe for KARA", in *Proc. IPAC'21*, Campinas, Brazil, May 2021, pp. 2039-2042. doi:10.18429/JACoW-IPAC2021-TUPAB251

[11] Inovesa, https://github.com/Inovesa

[12] P. Schönfeldt *et al.*, "Parallelized Vlasov-Fokker-Planck solver for desktop personal computers", *Phys. Rev. Accel. Beams*, vol. 20, p. 030704, 2017. doi:10.1103/PhysRevAccelBeams.20.030704

[13] J. B. Murphy, R. L. Gluckstern, and S. Krinsky, "Longitudinal wakefield for an electron moving on a circular orbit", in *Part. Accel.*, vol. 57, 1997. https://cds.cern.ch/record/1120287/

[14] M. Brosi *et al.*, "Fast Mapping of Terahertz Bursting Threshold and Characteristics at Synchrotron Light Sources", *Phys. Rev. Accel. Beams*, vol. 19, p. 110701, 2016. doi:10.1103/PhysRevAccelBeams.19.110701

[15] M. Brosi *et al.*, "Studies of the Micro-Bunching Instability in Multi-Bunch Operation at the KARA Storage Ring", in *Proc. IPAC'17*, Copenhagen, Denmark, May 2017, pp. 3645–3648. doi:10.18429/JACoW-IPAC2017-THOBA1

[16] M. Brosi, "In-Depth Analysis of the Micro-Bunching Characteristics in Single and Multi-Bunch Operation at KARA", PhD thesis, Institut für Beschleunigerphysik und Technologie, KIT, 2020. doi:10.5445/IR/1000120018